Crack tip strain evolution and crack closure during overload of a growing fatigue crack

De-Qiang Wang, Ming-Liang Zhu, Fu-Zhen Xuan
Key Laboratory of Pressure Systems and Safety, MOE; School of Mechanical and Power Engineering, East China University of Science & Technology, Shanghai 200237, China
mlzhu@ecust.edu.cn

Jie Tong
Mechanical Behavior of Materials Laboratory, School of Engineering, University of Portsmouth, Portsmouth PO1 3DJ, UK

ABSTRACT. It is generally accepted that fatigue crack growth is retarded after an overload, which has been explained either by plasticity-induced crack closure or near-tip residual stress. However, any interpretation of overload effect is insufficient if strain evolution in front of crack tip is not properly considered. The current understanding of overload-induced retardation lacks the clarification of the relationship between crack closure at crack wake and strain evolution at crack tip. In this work, a material with low work hardening coefficient was used to study the effect of overload on crack tip strain evolution and crack closure by in-situ SEM observation and digital image correlation technique. Crack opening displacement (COD) and crack tip strain were measured before and after the overload. It was observed that the evolution of crack tip strain follows the crack opening behaviour behind the crack tip, indicating a smaller influence of overload on micro-mechanical behaviour of fatigue crack growth. After the overload, plastic strain accumulation was responsible for crack growth. The strain at a certain distance to crack tip was mapped, and it was found that the crack tip plastic zone size correlated well with crack growth rate during post-overload fatigue crack propagation.

KEYWORDS. In-situ SEM; Overload; Fatigue crack growth; Digital image correlation.

OPEN ACCESS

Citation: Wang, D.-Q., Zhu, M.-L., Xuan, F.-Z., Tong, J., Crack Tip Strain Evolution and Crack Closure during Overload of a Growing Fatigue Crack, Frattura ed Integrità Strutturale, 41 (2017) 143-148.

Received: 28.02.2017
Accepted: 15.04.2017
Published: 01.07.2017

INTRODUCTION

Overloading behavior of a material has been widely investigated as variable amplitude loading is the load form that engineering structures and components often undergo. It is generally accepted that overloading of a fatigue crack often induces crack growth retardation and thus can influence fatigue life. To date, a variety of experimental and simulation work have focused on the influence of overload parameters, e.g. overload ratio, base stress intensity factor range, crack length, etc., on fatigue crack growth rates. Although several mechanisms for the retardation have been proposed, including crack closure [1-4], crack tip hardening [5], crack branching [6], residual stresses [7] or combined effects [5, 8], the micro-mechanical behavior of the overload is still an open issue. The crack closure concept, though extensively applied with its roles recognized in the overload process, is actually physical only at crack wake; whereas the driving part of crack growth and associated cracking of materials is at crack front. It seems that any interpretation of overload effect is insufficient if crack closure at crack wake is not correlated with cracking process in front of crack tip.

Digital image correlation (DIC) technique provides a good solution to strain measurement and has been widely applied in both engineering and laboratory scale researches. As for fatigue tests, the DIC method was found to be very helpful to the determination of plastic zone size [9], crack closure level [3, 4, 10, 11], and microstructural scale strain localization [12]. The DIC would be more powerful to resolve strain distribution if combined with high resolution images from SEM.

In this work, the DIC technique combined with in situ SEM was used to study the effect of overload on fatigue crack growth behavior. The strain evolution at crack tip as well as variation of crack opening displacement (COD) were measured and correlated with each other both before and after an overloaded growing fatigue crack. The driving force of fatigue crack growth in case of overload was also discussed.

EXPERIMENTAL METHODS

Material and specimen

The material used in this work is 25Cr2Ni2MoV, a type of rotor steel. The steel has been undergone quenching and tempering heat treatment, and a final tempering process was conducted at 560°C for 40 hours. The chemical composition of the steel in wt.% mainly includes C (0.18–0.27), Si (≤0.12), Mn (0.12–0.28), P (≤0.015), S (≤0.015), Ni (2.05–2.35), Cr (2.15–2.45), Mo (0.63–0.82), V (≤0.12), Cu (≤0.17) and Fe as the balance. The yield strength and ultimate strength of this steel are 793 MPa and 894 MPa, respectively. The material thus has a low work hardening coefficient. The microstructures are mainly tempered martensites.

Standard CT specimens with a /W ratio of 0.5 and a thickness B of 16 mm were firstly prepared and then pre-cracked using high frequency fatigue testing machine. The stress intensity factor range ΔK during the pre-cracking process was decreased from 15 MPa·m$^{1/2}$ to 13.5 MPa·m$^{1/2}$ for a first fatigue crack extension of 1.5 mm, followed by another 10% load decrease for another 1.5 mm extension. In total, the pre-crack length was 3 mm. Several dog-bone shaped miniature specimens with a gauge cross-section of 0.5×4 mm^2 and a gauge length of 10 mm were then cut from the CT specimen by Electrical Discharge Machining (EDM) technique. The specimen for in-situ SEM fatigue test was thus prepared with a pre-crack length of 2.286 mm. The shape and dimensions of the standard CT specimen and a small size fatigue specimen is shown in Fig. 1.

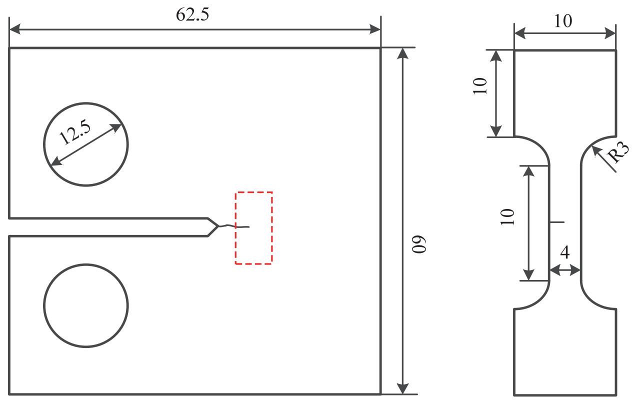

Figure 1: Shape and dimensions of standard CT specimen and the machined small size tensile specimen

In-situ fatigue test

Prior to in-situ fatigue test, the specimen was ground with SiC papers, and polished and chemically etched to reveal the microstructures and then mounted onto a Deben Microtest tensile module with a load capacity of 5 kN equipped into a SEM (Zeiss, EVO series). The loading scheme is shown in Fig. 2. The base line ΔK was 25 MP·m$^{1/2}$, and the overload ratio

(OLR) was set as 1.2. The cyclic loaded tests were interrupted every five cycles to take images, from which crack growth length and strain distribution were measured. SEM images were taken at two magnifications, i.e., 500X for strain measurement and 5000X for crack length measurement. As shown in Fig. 2, after 40 cycles of constant amplitude testing, an overload cycle was then exerted, followed by another 40 cycles of constant amplitude loading. Special attention was paid to the overload cycle, and the cycle just before and after the overload, by taking more images at an increment of 5% of P_{max}.

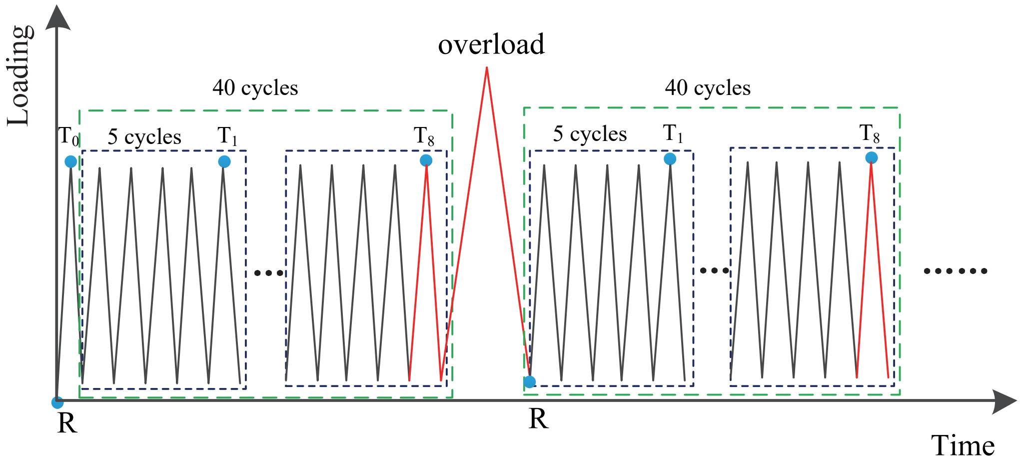

Figure 2: The loading scheme of the experiment (the 40 cycles before and after the overload cycle is a loading block contains 8 sub-block with 5 cycles for each of them)

Digital image correlation

The in-plane displacement and strain were analyzed by commercial DIC software (VIC-2D 2009, Correlated Solutions). The un-deformed image at zero load was set as the reference image and the deformed images were target ones. In this work, the intrinsic microstructures of the steel with an average characteristic size of 10 μm were regarded as speckles needed by DIC for tracking in-plane deformation. Suitable parameters such as subset size and step size were selected to be 31 pixels and 5 pixels, respectively. The strain measurement based on intrinsic microstructures as speckles was found with sufficient resolution in our previous work on a steel with similar microstructures [13].

RESULTS AND DISCUSSION

Crack growth morphologies

Fig. 3 shows the crack growth morphologies during the overload process and strain distribution based on DIC measurement. All the SEM images shown here are taken at peak load. The fatigue crack is just at a grain boundary before the overload cycle, as observed in Fig. 3a. The crack then gets across the grain boundary at the peak load of overloading and is branched (Fig. 3b). Fig. 3c shows the extension of branched cracks after overload cycle. Figs. 3d, 3e and 3f denote the strain distribution before, at and after the overload. The strain distribution near crack tip is varied, and the shape of highly concentrated zone from which plastic zone size is determined is also changed with overload. It seems that the strain is localized at and around the grain boundary, indicating the potential of next cracking under constant amplitude loading.

Crack tip strain evolution

The normal strains perpendicular to the crack plane ahead of the crack tip was extracted after correlation procedure. The reference image was taken at the minimum load at N_{OL}-1 cycle. The data points stands for the strain values with a distance of 50 μm away from the crack tip. The strain evolution during the three full cycles is shown in Fig. 4. Strain loops are observed in the pre-overload and post-overload cycle, while the overload induces large residual strain at the crack tip.

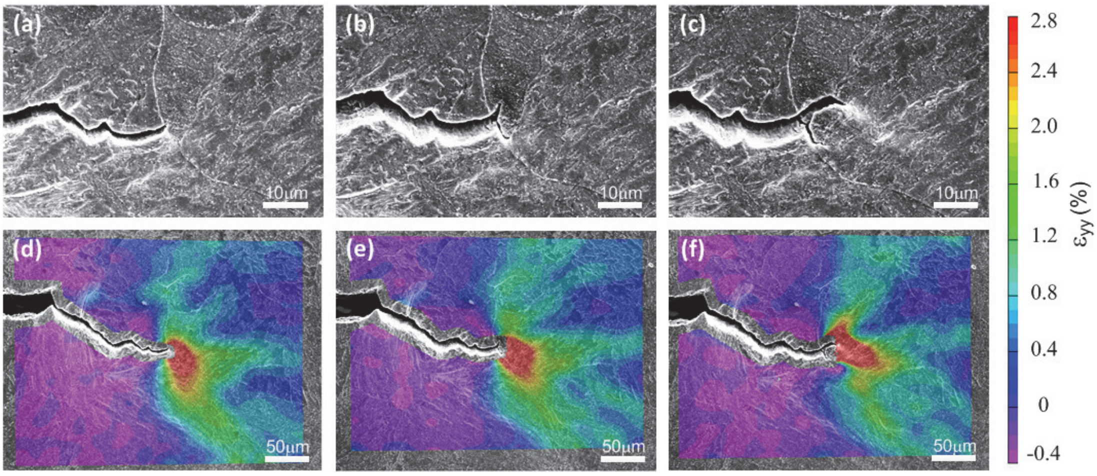

Figure 3: Crack growth morphologies during the overload process ((a), (b), and (c) are the crack tip before, at and after the overload, respectively; while (d), (e) and (f) are the corresponding strain distribution based on DIC measurement).

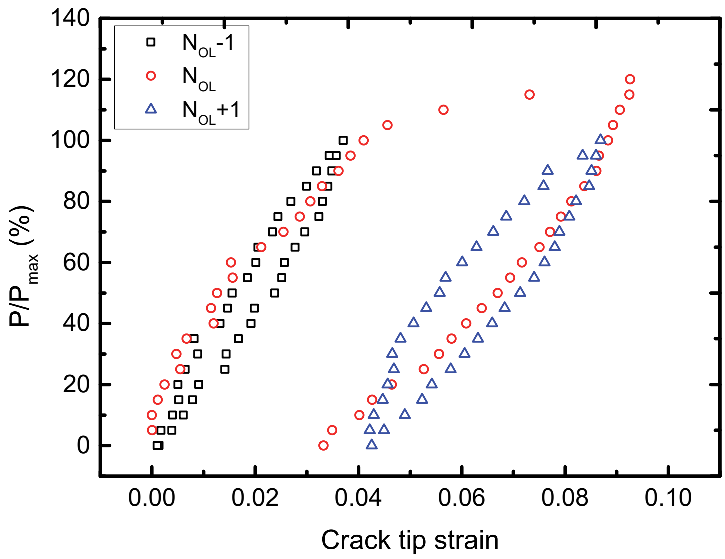

Figure 4: The strain evolution at the crack tip at OL-1, OL and OL+1 cycles (data points are extracted from the strain distribution with a distance of 50 μm in front of the crack tip)

Crack opening displacement evolution

Crack opening displacement (COD) values at crack wake was acquired by subtracting the vertical displacements of the top flank and bottom flank of the crack mouth, which varies as a function of distance behind the crack-tip [14]. In this study, the measurement point was 50 μm behind the crack-tip. The COD loops for the three full cycles, as shown in Fig. 5, have similar trend with that of crack tip strain in Fig. 3. It seems the loading process at the crack wake follows the mechanical response at the crack tip under the stress level in this work. As observed from Figs. 4 and 5, the crack closure varies little before and after the overload, probably due to the OLR is not very high, and the material investigated here has a low hardening coefficient.

Crack growth rate and plastic zone size

Apart from crack closure, other parameters, i.e., fatigue crack growth rate, plastic zone size and strain increasing rate, are calculated based on the experimental measurement, and the results are illustrated in Fig. 6. Strain increasing rate was defined as the slope of fitting curve of $\varepsilon_{max}/\varepsilon_0$ –N relationship, while plastic zone size was defined as areas where normal strain ε_{yy} is larger than 2%. Here, ε_{max} and ε_0 are the strain values at peak load and minimum load. It is observed that crack growth rate is decreased from 3.3×10^{-4} to 1.5×10^{-4} mm/cycle just after the overload, and then gradually restored to pre-overload level. It seems that the plastic zone size as compared with strain increasing rate is a better parameter for correlating crack growth rate.

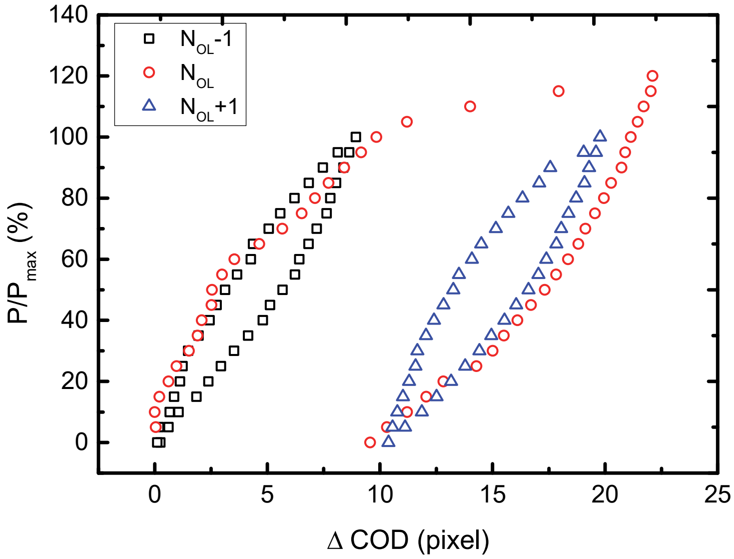

Figure 5: The evolution of COD at the crack wake at OL-1, OL and OL+1 cycles (data points are extracted from the measurement with a distance of 50 μm behind the crack tip)

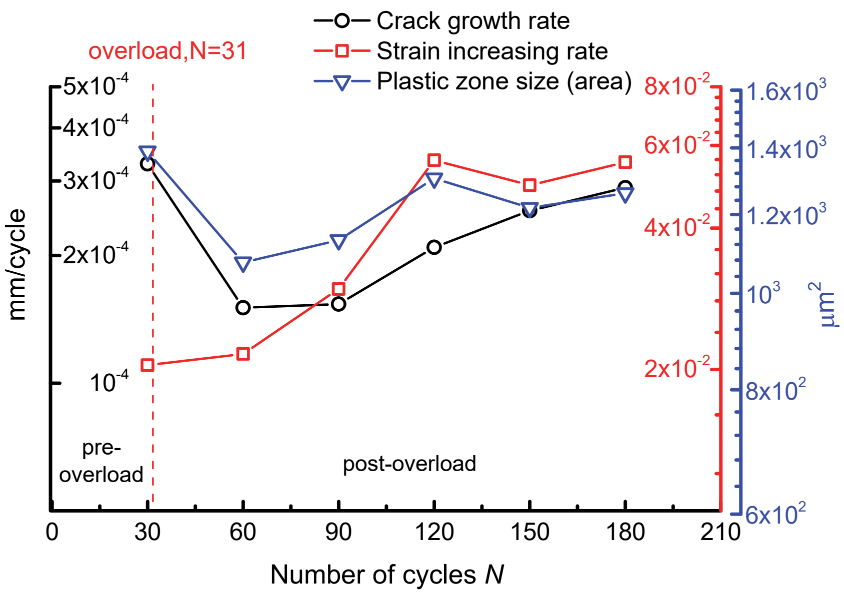

Figure 6: Variations of crack growth rate, strain increasing rate and plastic zone size with number of cycles

CONCLUSIONS

For the low hardening coefficient steel in this work, an in-situ fatigue test under an overload (OLR =1.2) revealed little influence of overload on fatigue crack growth behavior. The measured crack tip strain and crack opening displacement behind crack tip have similar response to external loading. Plastic zone size can correlate crack growth rate very well in case of overload.

ACKNOWLEDGEMENTS

The authors are grateful for the supports provided by the National Natural Science Foundation of China (Nos. 51575182 and 51325504).

REFERENCES

[1] Lee, S.Y., Choo, H., Liaw, P.K., An, K., Hubbard, C.R., A study on fatigue crack growth behavior subjected to a single tensile overload: Part II. Transfer of stress concentration and its role in overload-induced transient crack growth, Acta. Mater., 59 (2011) 495-502.
[2] Lee, S.Y., Liaw, P.K., Choo, H., Rogge, R.B., A study on fatigue crack growth behavior subjected to a single tensile overloadPart I. An overload-induced transient crack growth micromechanism, Acta. Mater., 59 (2011) 485-494.
[3] Nowell, D., de Matos, P.F.P., Application of digital image correlation to the investigation of crack closure following overloads, Procedia Engineering, 2 (2010) 1035-1043.
[4] Yusof, F., Lopez-Crespo, P., Withers, P.J., Effect of overload on crack closure in thick and thin specimens via digital image correlation, Int. J. Fatigue., 56 (2013) 17-24.
[5] Xiao, L., Ye, D., Chen, C., Liu, J., Zhang, L., Instrumented indentation measurements of residual stresses around a crack tip under single tensile overloads, Int. J. Mech. Sci., 78 (2014) 44-51.
[6] Suresh, S., Further remarks on the micromechanisms of fatigue crack growth retardation following overloads, Eng. Fract. Mech., 21 (1985) 1169-1170.
[7] Lopez-Crespo, P., Steuwer, A., Buslaps, T., Tai, Y.H., Lopez-Moreno, A., Yates, J.R., Withers, P.J., Measuring overload effects during fatigue crack growth in bainitic steel by synchrotron X-ray diffraction, Int. J. Fatigue., 71 (2015) 11-16.
[8] Sunder, R., Andronik, A., Biakov, A., Eremin, A., Panin, S., Savkin, A., Combined action of crack closure and residual stress under periodic overloads: A fractographic analysis, Int. J. Fatigue., 82 (2016) 667-675.
[9] Zhang, W., Liu, Y., Plastic zone size estimation under cyclic loadings using in situ optical microscopy fatigue testing, Fatigue. Fract. Eng. Mater. Struct., 34 (2011) 717-727.
[10] Carroll, J., Efstathiou, C., Lambros, J., Sehitoglu, H., Hauber, B., Spottswood, S., Chona, R., Investigation of fatigue crack closure using multiscale image correlation experiments, Eng. Fract. Mech., 76 (2009) 2384-2398.
[11] Nowell, D., Kartal, M.E., De Matos, P.F.P., Digital image correlation measurement of near-tip fatigue crack displacement fields: constant amplitude loading and load history effects, Fatigue. Fract. Eng. Mater. Struct., 36 (2013) 3-13.
[12] Stinville, J.C., Vanderesse, N., Bridier, F., Bocher, P., Pollock, T.M., High resolution mapping of strain localization near twin boundaries in a nickel-based superalloy, Acta. Mater., 98 (2015) 29-42.
[13] Wang, D.-Q., Zhu, M.-L., Xuan, F.-Z., Correlation of local strain with microstructures around fusion zone of a Cr-Ni-Mo-V steel welded joint, Mater. Sci. Eng. A, 685 (2017) 205-212.
[14] Zhu, M.-L., Xuan, F.-Z., Tu, S.-T., Observation and modeling of physically short fatigue crack closure in terms of in-situ SEM fatigue test, Mater. Sci. Eng. A, 618 (2014) 86-95.